Evaluating the Aerodynamic and Hydrodynamic Performance of Foil Geometries for Transmedium Applications Using Computational Fluid Dynamics

Peyton Cox

Spanish Fort High School

Author Note

This manuscript is a preprint, but has undergone and passed peer review by the Curieux Academic Journal. The author welcomes feedback from the scientific community.

Abstract

This study examines the impact of a foil's geometry on its efficiency in water and air to determine the optimal foil geometry for transmedium applications. Currently, there is no published research investigating the optimal transmedium foil geometry or comparing foil efficiency in air and water. This study intends to lay the groundwork for further research surrounding transmedium foils. The lift-to-drag ratios, lift coefficients, and drag coefficients were collected using NASA's simulation tool, FoilSim. Foils with diverse cambers and thicknesses were selected from the NACA four-digit family and tested in water and air at angles from 0° to 15° and speeds of 25 mph to 100 mph. The NACA 2408 was found to be the most efficient foil in four of the six scenarios, making it the optimal geometry for transmedium applications. The NACA 0008 was found to be the optimal geometry for a 5° angle of attack, and the NACA 0012 was determined to be the optimal geometry for 10° and 15° angles of attack. Developing research on transmedium foil geometries will enhance the viability of transmedium vehicles, which scientists and militaries worldwide are exploring for their applications in oceanography, warfare, and other fields. Additionally, the broad range of data tested in this study aims to narrow the scope that future researchers need to investigate to find the optimal transmedium geometry, allowing for more precise manipulation of variables while avoiding overly cumbersome data volumes.

Keywords: airfoil, hydrofoil, transmedium, lift, drag, naca, computational fluid dynamics, lift coefficient, drag coefficient, lift-to-drag ratio, aerodynamics, hydrodynamics

Evaluating the Aerodynamic and Hydrodynamic Performance of Foil Geometries for Transmedium Applications Using Computational Fluid Dynamics

Basic Fluid Dynamics and Phenomena

Fluid dynamics, the study of the flow of liquids and gases, is a complex field with many intricate definitions, principles, and phenomena. However, for the scope of this paper, we can condense it to a few key concepts related to the function of wings. Firstly, the two major forces acting on a wing are lift and drag. According to the world's leading organization on Aerodynamics, the National Aeronautics and Space Administration (NASA), lift is a force generated "by deflecting a moving fluid," resulting in an equal and opposite force (Benson, 2022). Wings typically deflect the fluid downward so that the lift force is directed upward. Air and sea crafts use this upward force to counteract their weight, allowing them to fly and increase their sailing speed, respectively. However, generating lift produces a corresponding drag force on the wing. NASA describes drag as an "aerodynamic force" caused by collisions between a "solid body [and] a fluid" that "[opposes] an aircraft's motion" (Hall, 2022). Since the goal of these crafts is to travel forward, designs typically aim to minimize this force to improve efficiency.

According to the Department Head of Fluid Dynamics at the Von Karman Institute, the forces of "Lift" and "drag [depend] linearly on the size of the object moving" and "the square of the relative velocity between the object" and the fluid (Arts et al., 2010, p. 51). Figure 1 shows the pressure distributions of these forces over the wing.

Figure 1

Illustration of Pressure Distributions Over an Airfoil

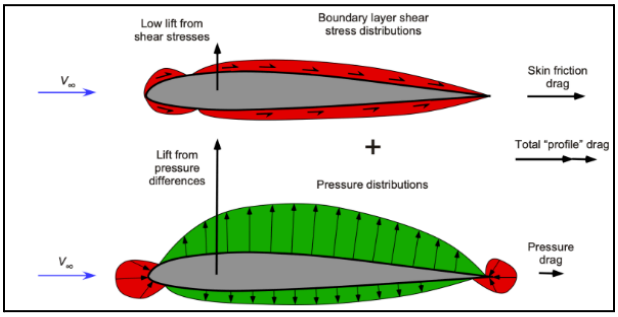

Note. From *Aerodynamics of airfoils. In Introduction to Aerospace Flight Vehicles (2nd ed.)*, by Leishman, J. G., 2023, Leishman, J. G., (https://doi.org/10.15394/eaglepub.2022.1066.n23). Copyright 2022–2025 by J. Gordon Leishman.

However, the magnitude of these forces depends on the characteristics of the surrounding fluid. For instance, density plays a key role in the strength of drag and lift forces. NASA found that "lift and drag depend linearly on the density of the fluid" because of "Newton's second law of motion," which states that force equals mass times acceleration (Benson, n.d.-a). This means that it requires more force to move a heavier fluid; consequently, increasing density increases lift because deflecting a heavier fluid generates a higher opposing force. However, it also increases drag because the larger inertia of the fluid exerts a greater force on the wing as it travels through it. According to Dr. Hepperle, Ph.D engineer with the German Aerospace Center, "water is 1000 times" denser than "air" (2021). Since lift and drag are directly proportional to the density of the surrounding fluid, the forces in water can be expected to be about one thousand times greater as well.

There are other differences between traveling through these fluids, as each has its own phenomenon associated with generating lift. However, to fully comprehend these phenomena, we first must understand precisely where they occur on the wing. According to Nuclear Power, a

non-profit educational engineering organization, the “region” where these appear is called the “boundary layer,” where the speed of the fluid “adjusts from zero velocity at the wall to [the] maximum [of] the mainstream… flow.” It forms as the wing cuts through a fluid, separating it from the surrounding flow. According to research by the German Institute of Fluid Mechanics, the boundary layer typically exists in two states, along the wing: “laminar [and] turbulent” (Schlichting & Gersten 29). These states have distinct characteristics that must be accounted for, due to their impact on the wing’s flight performance. Nuclear Power elaborates that “laminar” flow is “characterized” by “the streamwise velocity uniformly [changing],” while “turbulent” flow is “unstable” with “unsteady… swirling flows inside the boundary layer.” Generally, wings are designed to maintain smooth laminar flow over their surface, as it is more predictable and useful for generating lift.

Figure 2

Illustration of the Transition of the Boundary Layer from Laminar to Turbulent

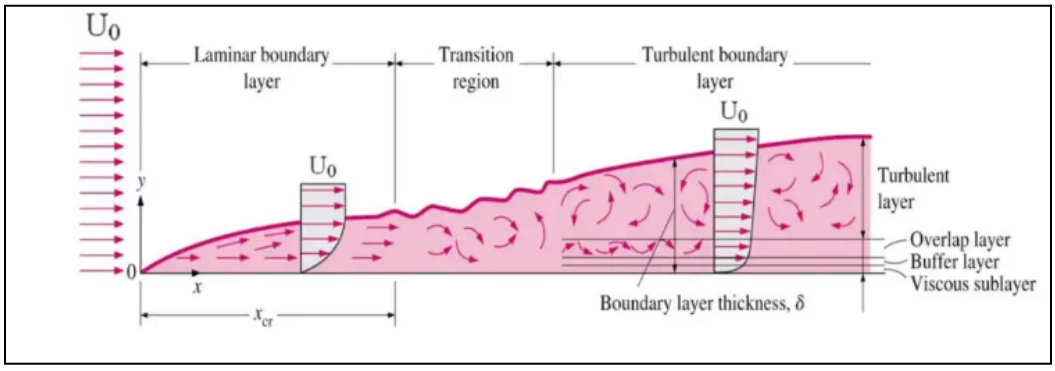

Note. From *Boundary Layer | Definition & Characteristics | Nuclear-power.com*, by Nuclear Power, (https://www.nuclear-power.com/nuclear-engineering/fluid-dynamics/boundary-layer/). Copyright 2025 by Nuclear Power.

Vortices from turbulent air can lead to a phenomenon known as stalling, where the boundary layer separates from the wing. Stalling typically occurs when the wing’s angle relative

to flow—known as the angle of attack (AoA)—becomes too high for the boundary layer to stay attached to the wing. According to a study from the International Journal of Mechanical Engineering, "With increasing AOA until AOA=15°, a further increase in AOA leads to a decrease in lift… due to the flow separation point [propagating] to the leading edge as the AOA increases" (Adel 30). Stalling not only decreases lift but also drastically increases drag. A study in the Journal of Aircraft found that when stalling, "the separation bubble and turbulent boundary-layer thickness both increase in size… resulting in increased parasitic drag." This is detrimental to the efficiency of wings and must be prevented.

While stalling also occurs in water, another phenomenon—cavitation—is more prominent and devastating to aquatic wings. Cavitation occurs "when water flows around" a wing and the "pressure drops below… the vapor pressure" causing "small vapor [bubbles] start to develop, which can grow into a large 'cave' of vapor." Similar to stalling, cavitation also "largely increases drag and… reduces lift," however, since "water is 1000 times" as dense, "the collapse of larger vapor bubbles may lead to vibrations and even structural damage." (Hepperle). This potential for damage makes it a much more serious problem than traditional stalling. When designing an aquatic wing, it can be accounted for by reducing the angle of attack or by minimizing the low-pressure gradient, ensuring that pressure along the wing stays above critical levels to prevent cavitation.

Figure 3

Illustration of the Effects of Increasing Angle of Attack on Fluid Separation

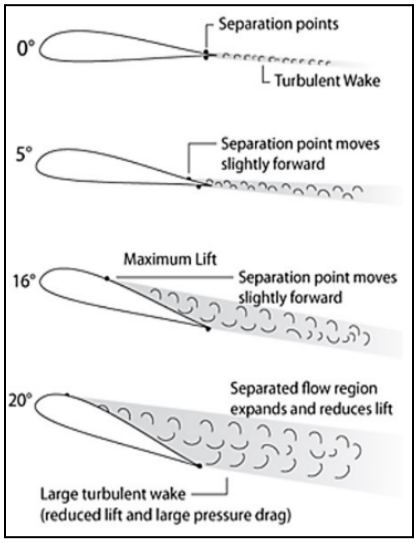

Note. From *How Does an Airplane Fly?*, by Arts, T., Asma, C., Corieri, P., De Pascale, N., Dobre, C., Kirmse, T., & Riethmuller, M., 2010, (https://www.scribd.com/document/612154552/How-to-fly-airplane). Copyright 2010 by von Karman Institute for Fluid Dynamics.

Standard Foil Design and Gap in Existing Comparative Studies

An airfoil is a specialized shape used by wings to maximize lift while minimizing drag, making them as efficient as possible. According to Dr. Hepperle, “Hydrofoils are like airfoils, just used in water... In most of these applications, a high lift-to-drag ratio is required” (2021). Hydrofoils also maximize efficiency; however, they are specifically designed to operate in the water. Since the general design concepts behind them are similar, the term “foil” will be used for generalization purposes. Some crucial terminology when describing a foil’s characteristics includes chord, camber, and maximum thickness. According to the Department of Mechanical Engineering at Necmettin Erbakan University, “chord is the connection line” between the front and rear edge of the foil, the “camber” is the “distance” between the center line and chord line, and “maximum thickness is the maximum distance between” the top and bottom of a foil (Kaya

et al., 2021, pp. 3–4). The chord is expressed as the length, while the thickness and camber—or concavity—are represented as percentages of the chord.

Many of these parameters are considered when designing foils for a specific purpose. For example, research from the National High School Journal of Science (NHSJS) found that sometimes "it is necessary to increase the camber of an airfoil," which "[increases] lift" at the cost of increased drag; similarly, "airfoil thickness" can be changed "to increase lift and drag" together (Punke, 2024). The effects of these changes are evident in Figures 4 and 5 and must be considered when designing a foil, particularly if versatility between fluids is required.

Figure 4

Graph Comparing the Lift/Drag Ratio as Camber Increases

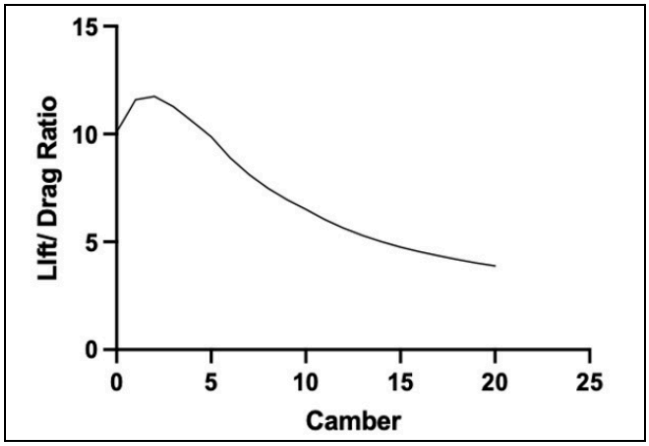

Note. The camber values in this graph are represented as a percentage of the chord. From *A review and study on Airfoils and aerodynamics*, by Punke, J. O., 2024, (https://nhsjs.com/2024/a-review-and-study-on-airfoils-and-aerodynamics). Copyright 2025 by The National High School Journal of Science.

Figure 5

Graph Comparing the Lift/Drag Ratio as Percent Thickness Increases

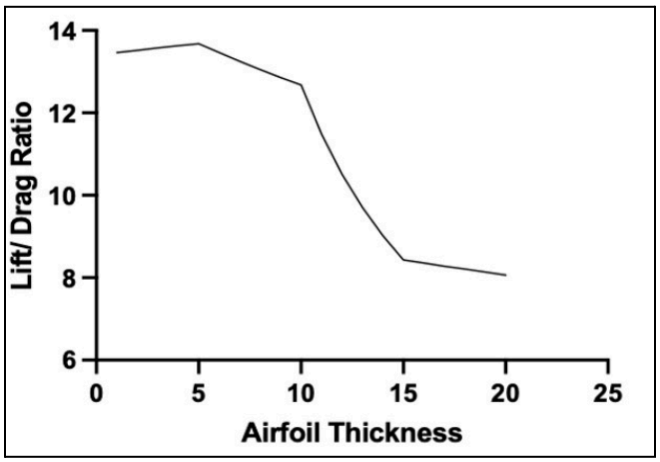

Note. The thickness values in this graph are represented as a percentage of the chord for a symmetrical airfoil. From *A review and study on Airfoils and aerodynamics*, by Punke, J. O., 2024, (https://nhsjs.com/2024/a-review-and-study-on-airfoils-and-aerodynamics). Copyright 2025 by The National High School Journal of Science.

Numerous studies have compared various types of foils against one another in real-world and computer-simulated tests. For example, a study from the Department of Mechanical Engineering at Necmettin Erbakan University tested multiple airfoil families, including the "NACA, FX, and S," and found the "NACA 6409, S 4110, and FX 60-157" airfoils had the highest lift coefficients and lift-to-drag ratios (Kaya et al., 2021, p. 10). These airfoils are moderately thick and highly cambered, optimized for air efficiency. Furthermore, a study from the International Journal of Mechanical Engineering found that when testing several airfoils at various angles of attack, the "SG6043 has the highest... lift-to-drag ratio" and "lift coefficient over the range of AOA." Conversely, they found that the "NACA 0012 airfoil has the lowest… lift coefficient and lift-to-drag ratio" (Adel, 2019, pp. 4–8). The SG6043 and the previously

mentioned airfoils suggest that moderate thickness and high camber are the optimal geometries for air efficiency. This trend is further supported by the inferior performance of the NACA 0012, a very thick and uncambered airfoil.

While these findings are helpful for designing airfoils, their generally thicker designs are likely poorly suited for use as hydrofoils because they would produce considerably more drag when cutting through water, a denser fluid. A study from Washington University in St. Louis found that "the hydrofoil for a sailing craft should have high lift at lower speeds and low drag at higher speeds" (Cocke, 2012, p. 1). These parameters necessitate finding a balance between making the hydrofoil thin enough to reduce drag, but thick and sufficiently cambered to produce significant lift. To achieve this balance, the study found that the optimal shape for aquatic efficiency is a thin, highly cambered hydrofoil, resembling the NACA 6606 (Cocke, 2012, p. 46). This design deviates from the trend observed in airfoils, where moderately thick designs achieve optimal efficiency.

Extrapolating to transmedium foil designs, such drastically different environments require exceptionally well-optimized geometries to generate sufficient lift in the air while significantly reducing their drag in the water to be practical in both fluids. Currently, there is no published research on this optimal design, nor are there any studies directly comparing designs in aquatic and aeronautical environments. My research aims to fill this gap by finding the most efficient geometry for a foil that balances its aquatic and aeronautical efficiency. To achieve this, I will examine the extent to which a foil's geometry impacts its performance in water and air comparatively. Based on the available research on airfoils and hydrofoils, I hypothesize that thin, moderately cambered foils will optimize performance for transmedium applications.

Methodology

Examining Standard Methods and Equations

In the scientific community, two primary methods are used to test the performance of foils: tunnel experiments and computational fluid dynamics (CFD). Tunnel experiments involve building a physical tunnel and testing model foils to collect real-world data on their performance. However, creating these tunnels is exceptionally challenging due to the complex design elements required to maintain laminar flow, physical limitations on the size and velocity, and the difficulty of measuring forces without affecting the results. These limitations are compounded by the time, resources, and expertise required to make them. Conversely, CFD offers a cheaper and quicker alternative for calculating the theoretical performance of foils by digitally simulating them. According to researchers at Dlubal, a structural analysis and design firm, "CFD is particularly valuable for design studies… and analyzing complex, dynamic scenarios that are difficult to replicate in a wind tunnel… [due to] its high flexibility and detail at lower running costs" (Kirova, 2025). My design study on foil geometries requires the flexibility and low cost that only CFD can provide, allowing for the collection of significantly more data. Furthermore, the American Institute of Aeronautics and Astronautics (AIAA) recognizes that "CFD can also predict performance under extreme velocity, pressure, and other conditions that wind tunnels cannot reproduce" (Stumpe, 2025). In conjunction with the research at Dlubal, the AIAA's conclusions support the use of CFD as a reliable and cost-effective method to test scenarios that would otherwise be impossible for my study to perform using tunnel experiments.

NASA FoilSim is a free simulator available on the NASA website that simulates foils under various conditions using CFD. According to research from the NHSJS, "FoilSim allows researchers to provide important variables" and "gather specific data" that have been "replicated

by other [experimental] studies' well-tested results" (Punke, 2024). It specifically allows for the manipulation of thickness, camber, angle of attack, velocity, fluid type, and more. Using the provided variables, FoilSim then calculates the lift-to-drag ratio (LTD) and the lift and drag coefficients. According to researchers in the Department of Mechanical Engineering at Necmettin Erbakan University, comparing the "lift [and drag] coefficients and lift-to-drag ratios… contributes to a better understanding of aerodynamic effects… assisting researchers when designing or selecting an airfoil" (Kaya et al., 2021, p. 3). These coefficients and ratios help represent the complex relationships between lift and drag for a given foil in a single number, without being dependent on scale; this allows for a broader understanding of the foil's performance, as it separates the results from a specific wing design, converting them into unitless values that make the data more generalizable to practical scenarios.

Foil Selection

Foils are typically divided into "families." These families share similar characteristics and naming methods. A study from the Department of Mechanical Engineering at Necmettin Erbakan University tested multiple airfoil families, including the "NACA, FX, and S," in search of the highest efficiency in air (Kaya et al., 2021, p. 1). The NACA family is the most popular of the airfoil families due to its long history and standardization. While there are multiple NACA naming systems, the most common is the four-digit code, which indicates the maximum camber, its position, and the maximum thickness of a foil. In order to more easily compare the foils and limit experimental variables, I will exclusively test the four-digit NACA family. To further reduce variables, I will only include those with a maximum camber position of 40% of the chord. As a result, the two variables in the geometry I will test are camber and thickness.

NACA four-digit foils are designed for quick and easy identification of a foil's characteristics as a percentage of the chord. The first digit of the code represents the maximum camber, the second digit represents the position of maximum camber, and the last two digits represent the maximum thickness. However, the second digit represents position in tens of percent, and for uncambered foils, the value is always zero. Using the example in Figure 6, a NACA 2421 would be interpreted as a foil with 2% camber, located 40% down the chord, and a maximum thickness of 21%.

Figure 6

Depiction of the NACA Airfoil Naming System

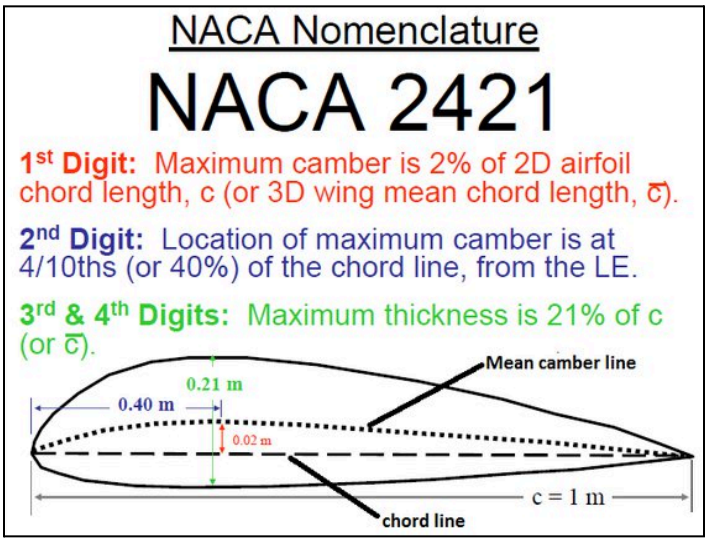

Note. From *Basic of Air foils, Aerodynamics its Application and CFD Modelling*, by Pachpute, S., 2024, (https://cfdflowengineering.com/basic-of-airfoils-aerodynamics-its-application-and-cfd-modeling). Copyright 2024 by CFD Flow Engineering.

To properly determine the effects of an airfoil's shape on lift and drag in different fluids, I must test a wide variety of airfoils to represent the various geometries. To achieve this diversity, my experiment will include foils of four different cambers: 0%, 2%, 4%, and 6%. Furthermore, they will have three different thicknesses: 4%, 8%, and 12%. Combining these factors will result

in twelve foils—shown in Figure 7—of varying thicknesses and cambers, representing a broad range of geometries.

Figure 7

Depiction of the Twelve Foils Tested

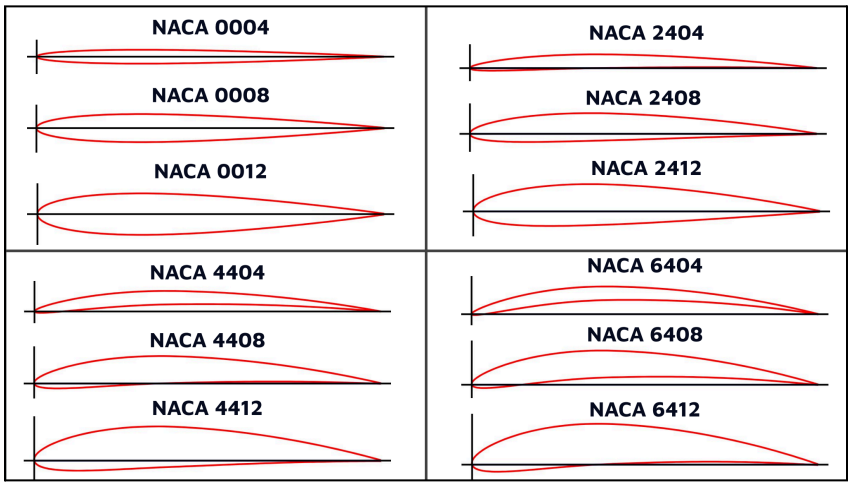

Note. Images generated using the *NACA 4-digit airfoil generator*, by Airfoil Tools. Copyright 2025 by Airfoil Tools

Experimental Method

The foundation of my research relies on determining each foil's lift-to-drag ratios, as it represents how efficiently a foil can generate lift while minimizing drag. According to a study in the International Journal of Mechanical Engineering, "The angle of attack has a direct impact on the lift and drag coefficients. For the lift coefficient, the maximum value occurred at an angle of attack of 15°. For the drag coefficient, the maximum value occurred at an angle of attack of 0°" (Adel, 2019). Since the lift-to-drag ratio is directly proportional to the quotient of lift and drag, efficiency also changes as the angle of attack varies; therefore, testing them at various angles—0°, 5°, 10°, and 15°—helps assess their overall performance in additional scenarios.

Varying velocity also affects foil efficiency. Research from the NHSJS found that "as speed increased, the lift and drag increased proportionally… producing dramatically more force" (Punke, 2024). Therefore, testing them at multiple speeds is also necessary to determine if a foil is broadly optimized for practical operations. The foils were tested at three speeds relevant to real-world aeronautical and hydronautical applications: 25 mph, 50 mph, and 100 mph. According to Candela—a leading hydrofoil manufacturer—most hydrofoil boats have a takeoff speed of 25 mph, and some can go up to 50 mph (Hosseini, 2024). Additionally, a researcher from Washington University in St. Louis tested hydrofoils at speeds of approximately 25 and 50 mph in their study on hydrofoil optimization (Cocke, 2012, p. 46). Furthermore, according to Embry-Riddle Aeronautical University, the Cessna 172 is the most widely produced general aviation aircraft in history, and has a minimum airspeed of approximately 50 mph and a takeoff speed of around 100 mph. Moreover, when researching airfoil geometries, the NHSJS study tested them at 100 mph (Punke, 2024). Taking all these factors into account, these three speeds encompass a range of critical speeds identified in studies and scenarios—especially at the overlap of 50 mph—where both airfoils and hydrofoils are known to operate.

To conduct my experiment, I used NASA FoilSim (NASA Glenn Research Center, 2024) to digitally simulate 24 different scenarios for each foil, resulting in nearly 300 total scenarios tested. From each of these simulations, I recorded the lift-to-drag ratios and the lift and drag coefficients, resulting in almost 900 total data points, organized in Appendices A through F. Following the NHSJS's example, I kept all simulation parameters to their default settings unless they were being directly tested. I compiled all my data into a Google Sheets document, where I then analyzed the values and created graphs to illustrate them.

Results

Wind Tunnel Simulation Results

Coefficient of Lift

Figure 8

Graph of the Coefficient of Lift From All Trials

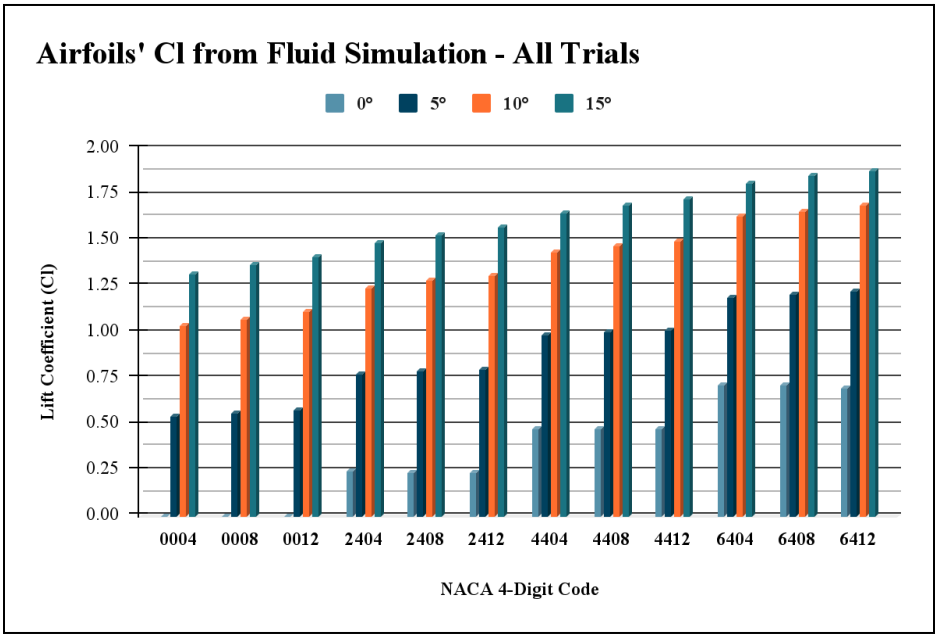

Note. Since uncambered airfoils deflect air symmetrically at 0° angle of attack, the lift coefficient and LTDs for these airfoils at that angle are zero and therefore not included in the description of any trends. Additionally, when analyzing changes in data, the numbers have been approximated for simplicity and clarity. The lift coefficients for all trials are illustrated in Figure 6, and all data from the wind tunnel simulations are presented in Appendices A, C, and E.

One of the most surprising trends in my experiment was that the coefficients of lift (Cl) remained constant across all trials for each foil. The fluid's speed and density did not affect the lift coefficient, only the angle of attack and foil geometry. Increasing the angle of attack made the most considerable impact on the lift coefficient; the first two increases—from 0° to 5° and 5°

to 10°—caused the lift coefficient to rise by 0.5, with the third increase—from 10° to 15°—causing it to rise by 0.25. The exact change in values varied, but most were within 0.05 of the approximate difference, excluding the airfoils with 6% camber that experienced a 0.15 increase in the lift coefficient from 10° to 15°. Additionally, at 0°, increasing thickness had little to no effect on the lift coefficient, decreasing it by only 0.01 between the NACA 2404 and 2408, as well as between the NACA 6408 and 6412. For 5° AoA, increasing thickness only caused a minute increase of 0.01 to 0.02 in the lift coefficients. However, the difference was more significant at 10° and 15°, ranging from an increase of 0.03 to 0.05. Notably, the less camber an airfoil had, the more substantial the increase in the lift coefficient was, with increasing angle and thickness. Conversely, increasing the camber at a given angle resulted in a relatively consistent increase in lift coefficients for all thicknesses: 0.25 for 0 °, 0.2 for 5° and 10°, and 0.15 for 15°.

Coefficient of Drag

Unlike the lift coefficient, the drag coefficient is dependent on the speed of the surrounding fluid, making the corresponding trends much more complex with the addition of another variable. However, many of the trends observed for the lift coefficient can be applied similarly to the drag coefficient; for example, raising the angle of attack had the most considerable impact on the drag coefficient, consistently leading to a substantial increase. From 0° to 5°, the drag coefficient increases by approximately 0.04 for airfoils with 0% camber, 0.07 for 2% camber, 0.09 for 4%, and 0.11 for 6% camber. From 5° to 10°, the drag coefficient increases by approximately 0.11 for airfoils with 0% camber, 0.13 for 2% camber, 0.15 for 4%, and 0.16 for 6% camber. From 10° to 15°, the drag coefficient increases by approximately 0.13 for airfoils with 0% and 2% camber, and by 0.12 for airfoils with 4% and 6% camber.

Additionally, increasing thickness had only a minute effect on the drag coefficient. At 0° and 5°, most cambered airfoils experienced an initial reduction of 0.003 between 4% and 8% thickness, followed by an increase of 0.003 between 8% and 12%. However, the change became more significant at 10° and 15°, with an initial considerable decrease of 0.010, followed by another decline of 0.005. Though at 15°, airfoils with 4% and 6% camber showed an exceptional reduction of nearly 0.025. Furthermore, increasing the camber at 0° and 5° resulted in a consistent increase in the difference between drag coefficients for all thicknesses, with 0.01 added per increase in camber for 0° and 0.005 for 5°. This trend continues for 10° and 15°, with a 0.005 increase in the difference between drag coefficients per increase in camber. However, thin airfoils (4%) break this trend by initially exhibiting a rise in the difference between drag coefficients of 0.005, followed by a decrease of 0.01. An important fact to note—due to the complexity of the camber's trend—is that I am referring to how the change, or difference, in the drag coefficient is changing with increasing camber, not how the drag coefficient itself is changing.

Finally, increasing speed caused a minor reduction in the drag coefficient; from 25 mph to 50 mph and 50 mph to 100 mph, the drag coefficient decreased by 0.001 to 0.003 for 0° and 5° AoA, 0.005 for 10°, and 0.009 for 15°.

Lift-to-Drag Ratio

Due to efficiency's relationship with the coefficients of lift and drag, the lift-to-drag ratio will have some of the most complex trends, demonstrating the patterns of both values. As the angle of attack increased, the airfoil's efficiency dramatically decreased. Unexpectedly, the airfoils that initially had less efficient designs had their lift-to-drag ratio reduced less than those that began with highly efficient designs. From 0° to 5°, the lift-to-drag ratio decreased by 3.50

for airfoils with 2% camber, 4.90 for 4% camber, and 3.50 for 6% camber; the NACA 2412 is an exception, with its efficiency decreasing by only 1.30. From 5° to 10°, the lift-to-drag ratio decreased by 3.90 for airfoils with 0% camber, 3.00 for 2% camber, 2.30 for 4% camber, and 1.80 for 6% camber. Finally, from 10° to 15°, the lift-to-drag ratio decreased by 2.10 for airfoils with 0% camber, 1.40 for 2% camber, 1.00 for 4% camber, and 0.80 for 6% camber. Increasing thickness from 4% to 8% at 0° and 5° tended to increase the efficiency of the airfoil, anywhere from 0.10 to 1.4, depending on the camber. Raising it further from 8% to 12% at 0° and 5° produced the opposite effect, reducing the efficiency by as much as 2.3. However, increasing the thickness to 12% became beneficial at 10° and 15°, with efficiency increasing by up to 0.60. Moderately thick airfoils consistently performed the best, except at high angles, where thick airfoils are necessary for optimal performance. Additionally, increasing thickness tended to grant higher efficiency boosts to airfoils with less camber. Finally, increasing speed caused a slight increase in the efficiency of the airfoils. Notably, the less camber and thickness an airfoil had, the more significant the increase in efficiency was at higher speeds. From 25 mph to 50 mph and 50 mph to 100 mph, the airfoils' lift-to-drag ratio at 0° increased by 0.70 for those with light camber, 0.5 for those with moderate camber, and 0.25 for those with heavy camber. As the angle increases, the range of efficiency gains from speed decreases; at 5°, the lift-to-drag ratio of airfoils with little to no camber only increases by 0.3, while those with moderate to heavy camber increase by 0.15. Likewise—at 10° and 15°—the efficiency of airfoils with little to no camber increases by 0.14, while those with moderate to heavy camber increase by 0.10.

At 25 and 50 mph in the air, the three most efficient airfoils in order were the NACA 4408, 2408, and 4412, with respective average lift-to-drag ratios of 13.60, 13.10, and 12.70. However, at 100 mph, the three most efficient airfoils in order were the NACA 2408, 4408, and

2404, with respective average lift-to-drag ratios of 14.20, 14.00, and 13.40. While those were the highest efficiency airfoils—overall and at 0°—as the angle increases the most efficient airfoils change: at 5° they become the NACA 0008, 0012, and 0004, at 10° they become the NACA 0012, 0008, and 0004, and at 15° they become the NACA 0012, 0008, and 2412. The only expectation is that at 25 mph at 10°, the NACA 2412 replaces the NACA 0004. The NACA 6404 was by far the worst-performing airfoil, having the worst efficiency at all angles and speeds.

Water Tunnel Simulation Results

Since the coefficient of lift is independent of the density of the surrounding fluid, it remains constant between the two experiments in water and air. Because it remains steady, I have omitted any descriptions of the results for the coefficients of lift, since they have already been covered in the previous section. Exact values and graphs for the water tunnel data can be found in Appendices B, D, and F.

Coefficient of Drag

Unlike the lift coefficient, the drag coefficient is dependent on the speed and density of the surrounding fluid. Since water has a density three orders of magnitude greater than air, this changes the values for the drag coefficients between the two fluids. However, the macro trends for the drag coefficient are consistent for both water and air.

Raising the angle of attack has the most considerable impact on the drag coefficient, always leading to a substantial increase. From 0° to 5°, the drag coefficient increases by 0.04 for hydrofoils with 0% camber, 0.06 for 2% camber, 0.09 for 4% camber, and 0.11 for 6% camber. From 5° to 10°, the drag coefficient increases by 0.10 for hydrofoils with 0% camber, 0.12 for 2% camber, 0.14 for 4% camber, and 0.15 for 6% camber. From 10° to 15°, the drag coefficient increases by 0.12 for hydrofoils with 0% camber, 0.11 for 2% and 4% camber, and 0.10 for 6%

camber. Additionally, increasing thickness had a slight effect on the drag coefficient. At 0° and 5°, almost all cambered hydrofoils experienced an initial reduction in the drag coefficient from 4% to 8% thickness of 0.003, followed by an increase when going from 8% to 12% thickness of 0.002. However, the change became more significant at 10° and 15°, with an initial moderate decrease of 0.006, followed by a minor reduction of 0.005. There was an exception at 15° with 4% and 6% cambered hydrofoils showing an unusually high decrease of nearly 0.020. Furthermore, increasing the camber at 0° and 5° resulted in a relatively consistent increase in the difference between drag coefficients for all thicknesses, with 0.01 being added per increase in camber for 0° AoA and 0.005 for 5°. For the higher angles of 10° and 15°, this trend continues with a 0.005 increase in the difference between drag coefficients per increase in camber; however, thin hydrofoils (4%) break this trend by having an initial increase in the difference between drag coefficients of 0.005, followed by a decrease of 0.01. An important fact to note—due to the complexity of the camber's trend—is that I am referring to how the change, or difference, in the drag coefficient is changing with increasing camber, not how the drag coefficient itself is changing.

Finally, increasing speed caused a minor reduction in the drag coefficient. From 25 mph to 50 mph and from 50 mph to 100 mph, the drag coefficient decreased by 0.001 to 0.003 for 0° and 5 ° AoA, 0.005 for 10°, and 0.007 for 15°.

Lift-to-Drag Ratio

Similarly to air, as the angle of attack increased, the hydrofoil's efficiency dramatically decreased. Unexpectedly, the hydrofoils that initially had less efficient designs had their lift-to-drag ratio reduced less than those that began with highly efficient designs. From 0° to 5°, the lift-to-drag ratio decreased by 5.20 for hydrofoils with 2% camber, 5.80 for 4% camber, and

3.90 for 6% camber; the NACA 2412 is an exception to this, with its efficiency only decreasing by 2.90. From 5° to 10°, the lift-to-drag ratio decreased by 4.60 for hydrofoils with 0% camber, 3.30 for 2% camber, 2.50 for 4% camber, and 1.90 for 6% camber. Finally, from 10° to 15°, the lift-to-drag ratio decreased by 2.20 for hydrofoils with 0% camber, 1.50 for 2% camber, 1.00 for 4% camber, and 0.80 for 6% camber. Increasing thickness from 4% to 8% at 0° and 5° tended to increase the efficiency of the hydrofoils, anywhere from 0.10 to 1.4, depending on the camber. Raising it further from 8% to 12% at 0° and 5° produced the opposite effect, reducing the efficiency by as much as 2.5. However, increasing the thickness to 12% became beneficial at 10° and 15°, with efficiency increasing by up to 0.40. Moderately thick hydrofoils consistently performed the best, except at high angles, where thick hydrofoils are necessary. Additionally, increasing thickness tended to grant higher efficiency boosts to hydrofoils with less camber. Finally, increasing the speed yielded a slight improvement in hydrofoil efficiency. Notably, the less camber and thickness a hydrofoil had, the more significant the increase in efficiency was at higher speeds. From 25 mph to 50 mph and 50 mph to 100 mph, the hydrofoils' lift-to-drag ratio at 0° increased by 0.70 for those with light camber, 0.40 for those with moderate camber, and 0.20 for those with heavy camber. As the angle increases, the range of efficiency gains from speed decreases; at 5°, the lift-to-drag ratio of hydrofoils with no camber increases by 0.30, while those with light camber increase by 0.20, and those with moderate to heavy camber increase by 0.10. Likewise—at 10° and 15°—the efficiency of hydrofoils with little to no camber increases by 0.11, while those with moderate to heavy camber increase by 0.09.

At 25 and 50 mph in the air, the three most efficient hydrofoils in order were the NACA 2408, 4408, and 2404, with respective average lift-to-drag ratios of 15.20, 14.60, and 14.40. However, at 100 mph, the three most efficient hydrofoils in order were the NACA 2408, 4408,

and 2404, with respective average lift-to-drag ratios of 12.70, 12.30, and 11.80. While those were the highest efficiency hydrofoils—overall and at 0°—as the angle increases the most efficient hydrofoils change: at 5° they become the NACA 0008, 0012, and 0004, at 10° they become the NACA 0012, 0008, and 0004, and at 15° they become the NACA 0012, 0008, and 2412. The only expectation is that at 50 and 100 mph at 0°, the NACA 2404 replaces the NACA 4408.

Cross-Analysis of Trends for Transmedium Applications

In both fluid simulations, increasing the angle of attack drastically reduced foil efficiency; therefore, all the highest-efficiency foils were found at 0°, as shown in Figure 9, which displays the top three.

Figure 9

Graph Comparing the Top Three Foils' Lift-to-Drag Ratios at 0° Angle of Attack

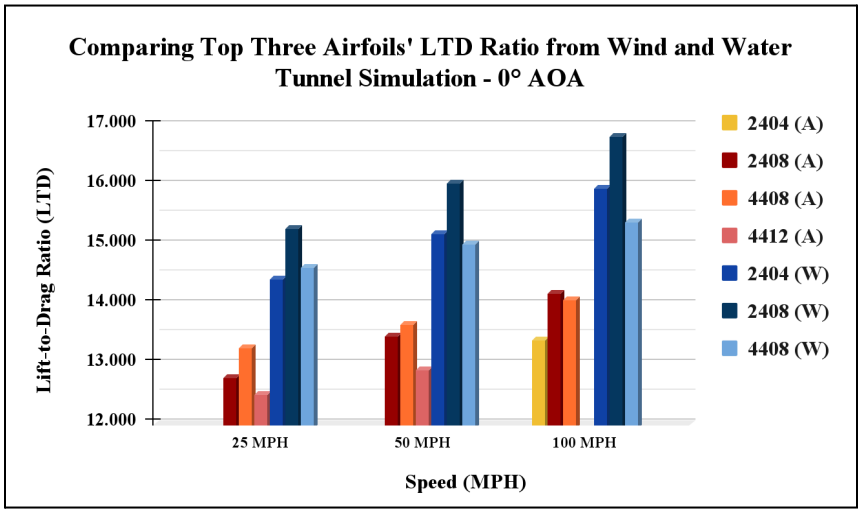

Note. The "A" represents the results from the trials performed in air, while the "W' refers to the trials conducted in water.

In water, the NACA 2408 always has the highest LTD, with the NACA 4408 having the second-highest at 25 mph, before being superseded by the NACA 2404. In the air, the NACA 4408 is the most efficient, except at 100 mph, when the NACA 2408 surpasses it. However, in all

scenarios, the NACA 4408 and 2408 take both first and second place. In both fluids, the NACA 2408 and 4408 appear to be the most efficient foils, allowing us to focus the analysis on these two.

Figure 10

Graph Comparing the Top Two Foils' Lift-to-Drag Ratios at Various Speeds

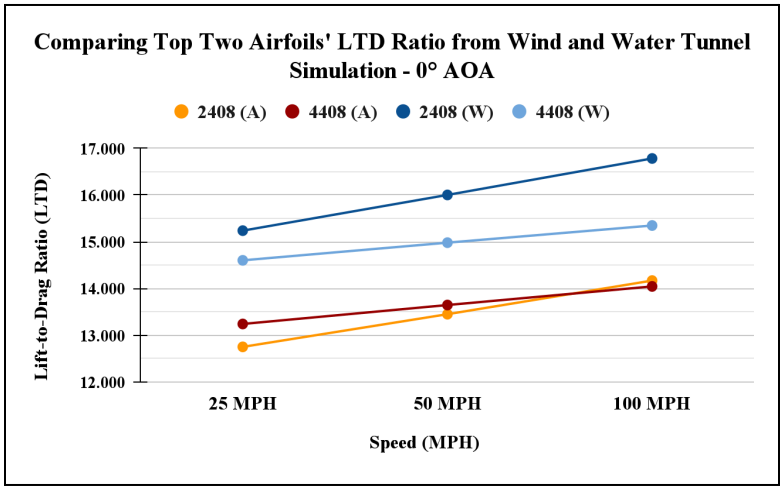

Figure 11

Graph Comparing the Top Two Foils' Lift-to-Drag Ratios Across All Trials

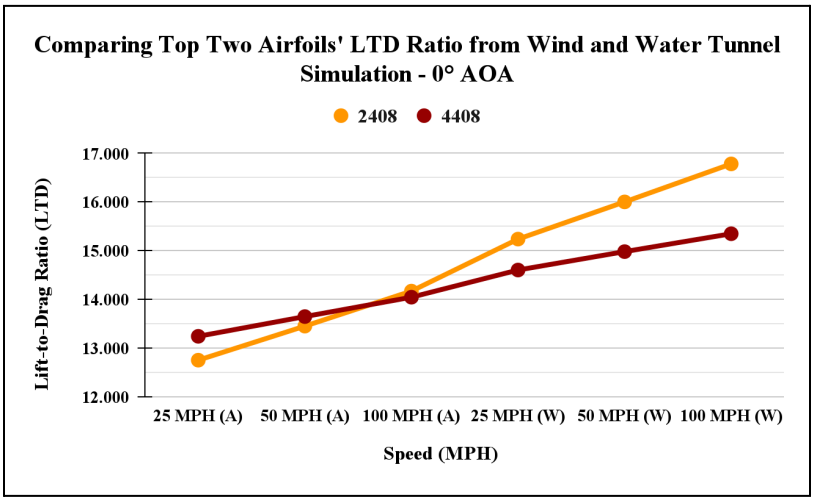

When directly comparing the two in Figures 10 and 11, the winner becomes apparent. In water, the NACA 2408 has a significant performance advantage that only widens as speed

increases. While the NACA 4408 initially outperforms the NACA 2408 in air, the gap closes at 50 mph, and the NACA 2408 surpasses it at 100 mph. Since the NACA 2408 is the most efficient foil in four of the six scenarios—only falling slightly behind in the other two—it is the optimal airfoil shape tested for transmedium applications, with an LTD of 12.8 to 16.8.

While the higher AoAs all have lower efficiencies than 0°, it is still worth analyzing the highest-performing foils because the higher AoA foils have larger lift coefficients, meaning that—for applications where more lift is needed—they may serve as alternatives. Unlike 0°, the other AoAs showed no fluctuation in the highest-performing foil across all trials. For 5°, the NACA 0008 was the most efficient, with an LTD of 11.2 to 13.0. For 10° and 15°, the NACA 0012 was the most efficient, with LTDs of 7.4 to 8.0 and 5.0 to 5.6, respectively.

These findings refute the hypothesis that thin, moderately cambered airfoils are optimal, suggesting that moderately thick, lightly cambered foils are the most efficient for transmedium applications. Furthermore, the findings from 10° and 15° refute Adel's conclusion that the NACA 0012 performs poorly, as it was the foil with the highest efficiency at both angles. Wind testing at 25 and 50 mph reinforces Kaya's claim that moderately thick airfoils are the most efficient; however, the results indicate that moderate camber performs better than the high camber found in the study.

Discussion

Fulfillment in the Gaps of the Research

This study addresses the significant lack of scholarly research on transmedium foils and their optimization. While airfoils are highly researched due to their central role in aviation, hydrofoils represent only a small share of the boating industry, resulting in limited research to advance the technology. With transmedium foils being a more niche combination of both airfoils

and hydrofoils, there is currently no public research on their optimization. This study, however, initiates the scholarly conversation for these specialized foils by postulating that the NACA 2408 is the most efficient foil for transmedium applications.

Practical Implications

While transmedium vehicles are quite niche and specialized compared to more common applications of foils—such as airplanes or hydrofoil boats—there has been some interest in their development in specific fields, particularly for military and ecological applications. For the military, transmedium vehicles offer a combination of stealth and flexibility that gives their design a tactical edge. The US government (Goddard & Eastgate, 2010), the Chinese government (Honrada, 2022), and many military contractors and research institutions have studied the efficacy of these vehicles and found them to have many benefits over traditional designs; however, between budget constraints, limited research, high complexity, and a lack of demand, many of these projects were never finalized or produced. Conversely, transmedium drones are being explored for ecological applications to enhance the survey and exploration of oceanic areas. Chinese researchers have developed a prototype drone, known as the TJ-FlyingFish, to demonstrate the effectiveness of a transmedium design compared to conventional underwater drones, which have a more limited range and survey capabilities (McMillan, 2023).

Research Limitations

As with all digital experiments, the data collected in this study is purely theoretical, as opposed to tunnel experiments that can provide more real-world, practical data. While NASA FoilSim has been validated through real-world experiments, the near-infinite number of possible configurations within the simulation means that not all of them have been verified. Furthermore, FoilSim is a simplified CFD model, which is why it is free, easily accessible, and requires no

specialized software or hardware to compute simulations. However, this also means that it is not as accurate as other CFD models, which can individually model the flow of thousands to even millions of particles.

Additionally, even though this study analyzed 12 different foils in 24 different scenarios, altering five independent variables and analyzing three dependent variables with a total data set nearing 900 values, the overall range of the tested variables was limited due to the impracticality of introducing more data points, as it would damage the depth of analysis. For instance, it is possible that the most efficient foil was NACA 3507; however, since this configuration falls between the selected intervals, it would be impossible to determine purely based on this study alone. Extrapolating further, the NACA 4-digit family may not be specific enough to fully describe the optimal geometry, and instead, it might be in another family, such as the NACA 5-digit, 6-digit, FX, S, etc.

Research Implications and Paths For Advancement

Validating the results of this study with high-fidelity CFD models or tunnel experiments would help verify that the NACA 2408 is the most widely efficient foil for transmedium applications. However, this study did not aim to precisely determine the optimal geometry, but instead to guide the scholarly conversation towards identifying the most efficient transmedium foil. Researchers can use the findings from this study as a stepping stone to narrow their search to high-performing foils, such as the NACA 2408 and 4408, while avoiding wasting time on foils that consistently perform poorly, like the NACA 6404. A narrower search allows for more specific manipulation of variables, testing smaller intervals of camber and thickness, or introducing camber position as another variable.

Furthermore, research into transmedium optimization could expand beyond the foils to other parts of these vehicles, such as the wings or body. While these components have simpler fluid interactions when compared to the lift-generating foils, the principles of maintaining smooth, low-drag flow are very similar. Researchers can utilize the findings from this study, which demonstrate that moderately thick designs are more efficient than thinner designs when considering the construction of these other elements.

References

Adel, M. (2019). A comparative study for different shapes of airfoils. In *International Journal of Mechanical Engineering* (Vol. 4). https://www.iaras.org/iaras/filedownloads/ijme/2019/012-0007(2019).pdf

Arts, T., Asma, C., Corieri, P., De Pascale, N., Dobre, C., Kirmse, T., & Riethmuller, M. (2010). *How does an airplane fly?* (By European Commission) [Book]. von Karman Institute for Fluid Dynamics. https://www.fp7-restarts.eu/images/pdf/book.pdf

Benson, T. (n.d.-a). *Density effects on aerodynamic forces*. NASA Glenn Research Center. https://www.grc.nasa.gov/www/k-12/VirtualAero/BottleRocket/airplane/density.html

Benson, T. (n.d.-b). *The lift equation*. NASA Glenn Research Center. Retrieved September 20, 2024, from https://www.grc.nasa.gov/www/k-12/VirtualAero/BottleRocket/airplane/lifteq.html

Boundary Layer | Definition & Characteristics | Nuclear-power.com. (2021, October 24). Nuclear Power. https://www.nuclear-power.com/nuclear-engineering/fluid-dynamics/boundary-layer/

Cocke, W. (2012). Shape Optimization of Hydrofoils. *Washington University All Theses and Dissertations (ETDs)*. https://doi.org/10.7936/k7sn0718

Embry-Riddle Aeronautical University. (n.d.). *Cessna 172*. https://daytonabeach.erau.edu/about/fleet-simulators/cessna-172

Goddard, R., & Eastgate, J. (2010). Submersible Aircraft Concept Design Study. *Naval Surface Warfare Center Carderock Division*. https://apps.dtic.mil/sti/pdfs/ADA554344.pdf

Hall, N. (2022, July 21). *What is Drag? | Glenn Research Center | NASA*. Glenn Research Center | NASA. https://www1.grc.nasa.gov/beginners-guide-to-aeronautics/what-is-drag/

Hepperle, M. (2021, May 18). *Hydroprops*. MH-Aerotools. Retrieved September 20, 2024, from https://www.mh-aerotools.de/airfoils/hydrofoils.htm

Honrada, G. (2022, September 17). China unveils supersonic missile-torpedo anti-ship weapon. *Asia Times*. https://asiatimes.com/2022/09/china-unveils-supersonic-missile-torpedo-anti-ship-weapon/

Hosseini, Y. (2024, July 8). *Foiling vs. Floating; Understanding the Differences Between Hydrofoil Boats and Other Boats*. Candela. https://candela.com/foiling-vs-floating-understanding-the-differences-between-hydrofoil-boats-and-other-boats/

Kaya, M. N., Kök, A. R., & Kurt, H. (2021). Comparison of aerodynamic performances of various airfoils from different airfoil families using CFD. *Wind and Structures*, *32*(3), 239–248. https://doi.org/10.12989/was.2021.32.3.239

Kirova, I. (2025, February 19). *CFD or wind tunnel? 6 Most important benefits of digital flow simulation for engineers*. Dlubal Software. https://www.dlubal.com/en/support-and-learning/support/knowledge-base/001912#:~:text=In%20summary%2C%20CFD%20is%20particularly,and%20performing%20accurate%20aerodynamic%20assessments.

Leishman, J. G. (2023). Aerodynamics of airfoils. In *Introduction to Aerospace Flight Vehicles* (2nd ed.). Embry-Riddle Aeronautical University. https://doi.org/10.15394/eaglepub.2022.1066.n23

McMillan, T. (2023, November 25). *Chinese engineers develop transmedium drone that can fly in the air and swim underwater*. The Debrief. https://thedebrief.org/chinese-engineers-develop-transmedium-drone-that-can-fly-in-the-air-and-swim-underwater/

NACA 4 digit airfoil generator (NACA 2412 AIRFOIL). (n.d.). http://airfoiltools.com/airfoil/naca4digit

NASA Glenn Research Center. (2024, July 17). *Student Airfoil Interactive | Glenn Research Center | NASA*. Glenn Research Center | NASA. https://www1.grc.nasa.gov/beginners-guide-to-aeronautics/foilsimstudent

Pachpute, S. (2024). Basic of Air foils, Aerodynamics its Application and CFD Modelling. *CFD Flow Engineering*. https://cfdflowengineering.com/basic-of-airfoils-aerodynamics-its-application-and-cfd-modeling/

Punke, J. O. (2024, August 3). *A review and study on Airfoils and aerodynamics - NHSJS*. NHSJS. https://nhsjs.com/2024/a-review-and-study-on-airfoils-and-aerodynamics//

Schlichting, H., & Gersten, K. (2016). Fundamentals of Boundary–Layer Theory. In *Springer eBooks* (pp. 29–49). https://doi.org/10.1007/978-3-662-52919-5_2

Stumpe, J. (2025, April 2). *Symbiosis: Why CFD and wind tunnels need each other*. Aerospace America. https://aerospaceamerica.aiaa.org/features/symbiosis-why-cfd-and-wind-tunnels-need-each-other/

Appendix

Appendix A: Tables and Graphs From 25 MPH Wind Tunnel Simulation Results

NACA Code	Cl at 0°	Cl at 5°	Cl at 10°	Cl at 15°	Cd at 0°	Cd at 5°	Cd at 10°	Cd at 15°
0004	0.00	0.54	1.04	1.32	0.011	0.053	0.166	0.292
0008	0.00	0.56	1.07	1.37	0.013	0.050	0.156	0.297
0012	0.00	0.58	1.11	1.41	0.018	0.053	0.150	0.282
2404	0.25	0.77	1.24	1.49	0.020	0.090	0.223	0.353
2408	0.24	0.79	1.28	1.53	0.019	0.086	0.213	0.342
2412	0.24	0.80	1.31	1.57	0.023	0.088	0.208	0.330
4404	0.48	0.99	1.44	1.65	0.041	0.134	0.286	0.418
4408	0.48	1.00	1.47	1.69	0.036	0.130	0.275	0.391
4412	0.48	1.01	1.50	1.73	0.038	0.130	0.272	0.382
6404	0.71	1.19	1.63	1.81	0.073	0.179	0.341	0.473
6408	0.71	1.21	1.66	1.85	0.068	0.178	0.337	0.448
6412	0.70	1.22	1.69	1.88	0.068	0.181	0.340	0.446

NACA Code	LTD at 0°	LTD at 5°	LTD at 10°	LTD at 15°
0004	0.000	10.197	6.259	4.535
0008	0.000	11.205	6.875	4.601
0012	0.000	10.876	7.358	4.983
2404	12.005	8.565	5.570	4.219
2408	12.752	9.110	5.993	4.474
2412	10.480	9.096	6.272	4.751
4404	11.803	7.348	5.031	3.950
4408	13.242	7.694	5.343	4.324
4412	12.463	7.776	5.518	4.523
6404	9.748	6.670	4.783	3.825
6408	10.441	6.782	4.930	4.127
6412	10.355	6.751	4.962	4.223

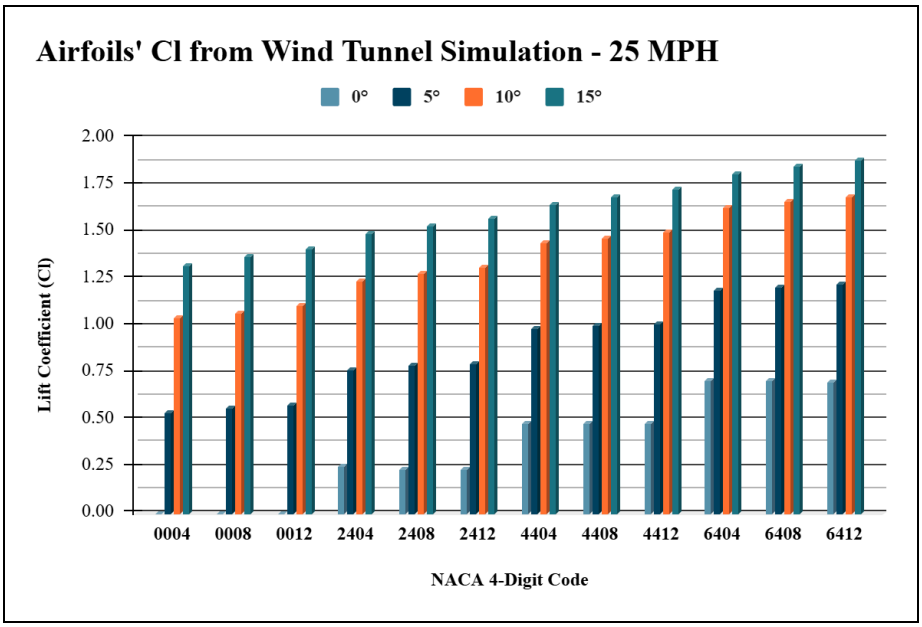
Airfoils' Cl from Wind Tunnel Simulation - 25 MPH
0°
5°
10°
15°
Lift Coefficient (Cl)
2.00
1.75
1.50
1.25
1.00
0.75
0.50
0.25
0.00
0004
0008
0012
2404
2408
2412
4404
4408
4412
6404
6408
6412
NACA 4-Digit Code

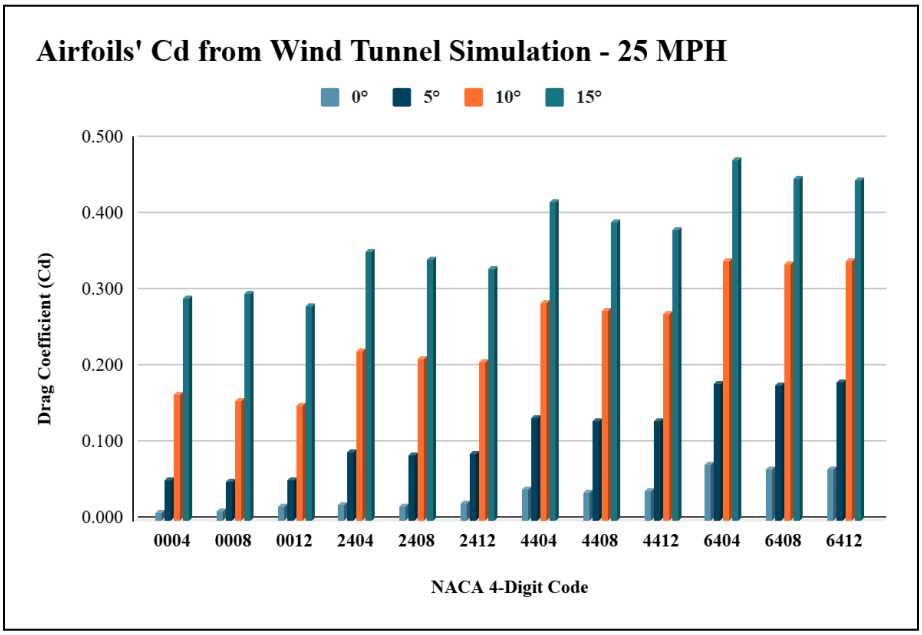
Airfoils' Cd from Wind Tunnel Simulation - 25 MPH
0°
5°
10°
15°
Drag Coefficient (Cd)
0.500
0.400
0.300
0.200
0.100
0.000
0004
0008
0012
2404
2408
2412
4404
4408
4412
6404
6408
6412
NACA 4-Digit Code

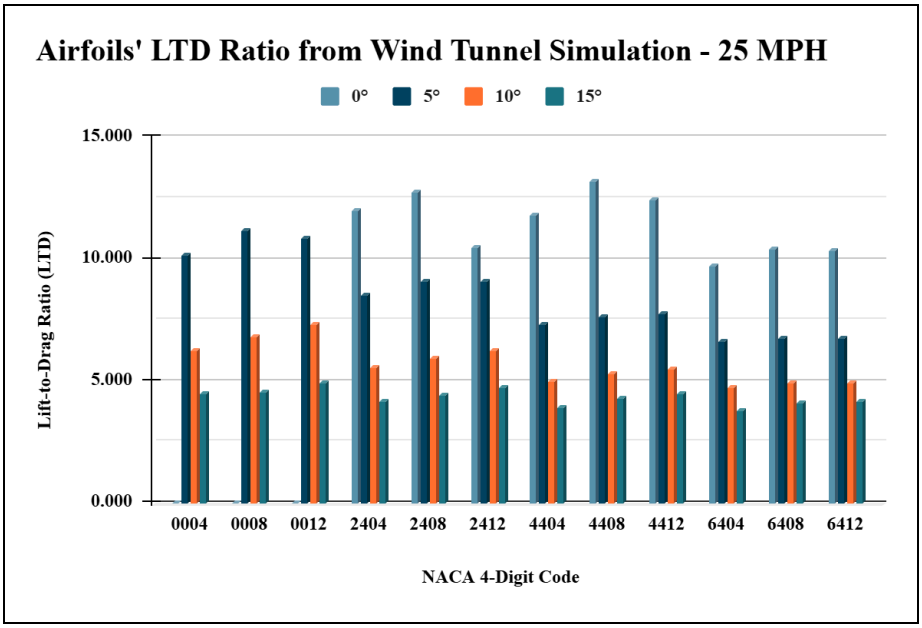

Appendix B: Tables and Graphs From 25 MPH Water Tunnel Simulation Results

NACA Code	Cl at 0°	Cl at 5°	Cl at 10°	Cl at 15°	Cd at 0°	Cd at 5°	Cd at 10°	Cd at 15°
0004	0.00	0.54	1.04	1.32	0.008	0.047	0.151	0.262
0008	0.00	0.56	1.04	1.32	0.010	0.046	0.145	0.269
0012	0.00	0.58	1.11	1.41	0.014	0.048	0.142	0.260
2404	0.25	0.77	1.24	1.49	0.017	0.082	0.205	0.320
2408	0.24	0.79	1.28	1.53	0.016	0.080	0.199	0.314
2412	0.24	0.80	1.31	1.57	0.019	0.082	0.197	0.307
4404	0.48	0.99	1.44	1.65	0.036	0.124	0.265	0.381

4408	0.48	1.00	1.47	1.69	0.033	0.122	0.259	0.363
4412	0.48	1.01	1.50	1.73	0.034	0.123	0.258	0.358
6404	0.71	1.19	1.63	1.81	0.067	0.168	0.320	0.435
6408	0.71	1.21	1.66	1.85	0.063	0.169	0.319	0.418
6412	0.70	1.22	1.69	1.88	0.063	0.171	0.323	0.419

NACA Code	LTD at 0°	LTD at 5°	LTD at 10°	LTD at 15°
0004	0.000	11.467	6.878	5.045
0008	0.000	12.372	7.402	5.084
0012	0.000	12.006	7.784	5.412
2404	14.409	9.395	6.061	4.661
2408	15.238	9.859	6.413	4.877
2412	12.712	9.814	6.628	5.106
4404	13.226	7.938	5.434	4.339
4408	14.603	8.223	5.689	4.663
4412	13.881	8.274	5.820	4.822

6404	10.608	7.086	5.099	4.163
6408	11.241	7.167	5.211	4.418
6412	11.177	7.127	5.223	4.488

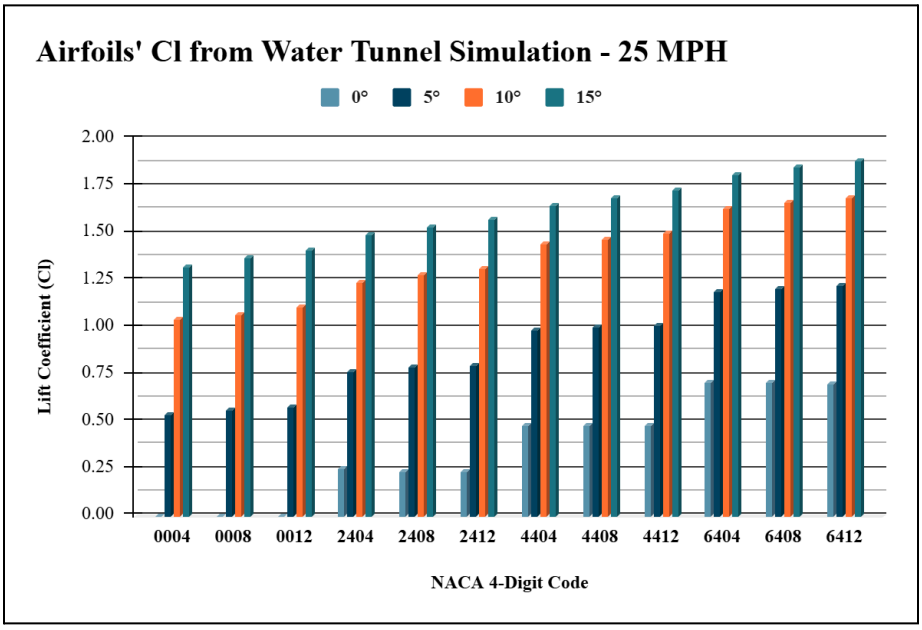

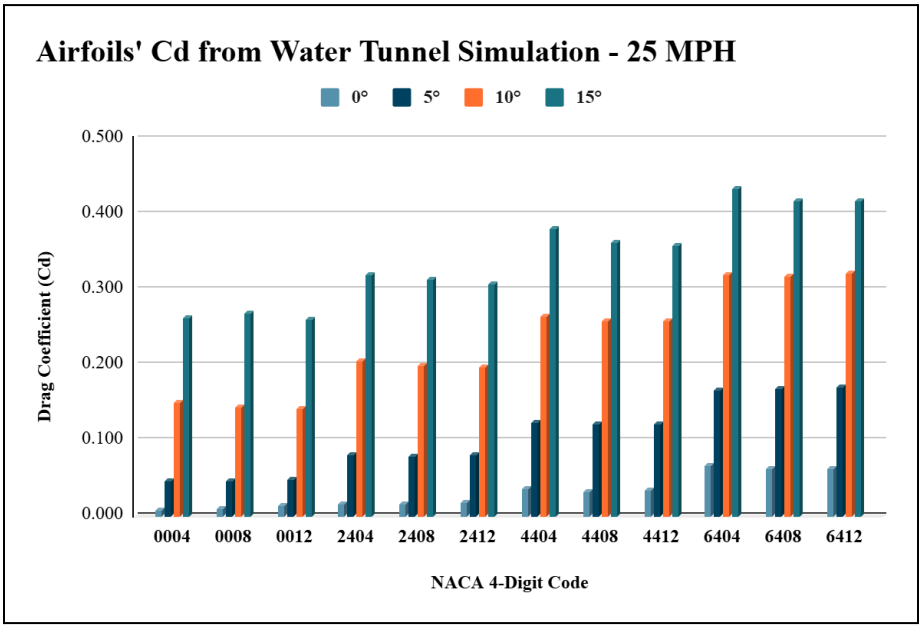

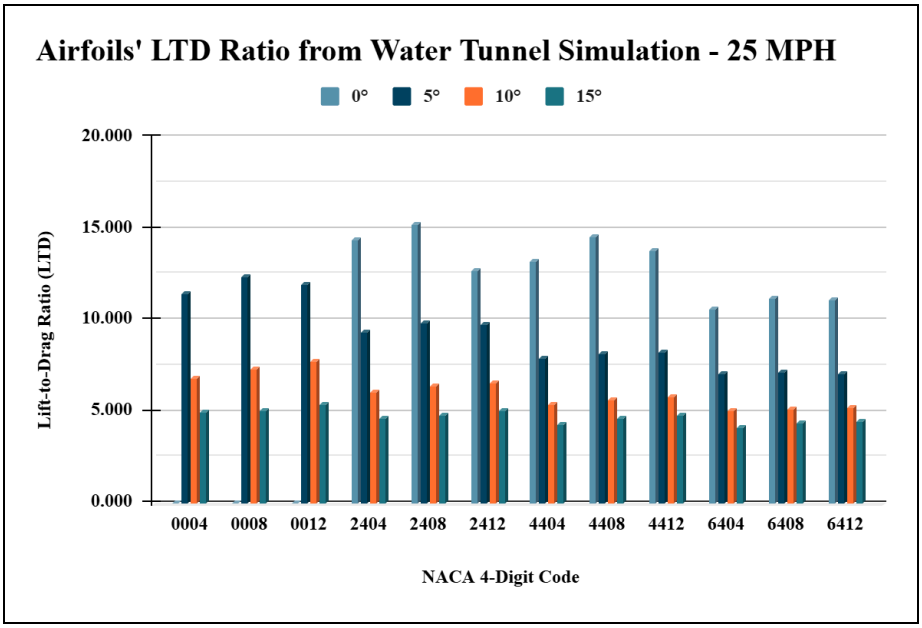

Appendix C: Tables and Graphs From 50 MPH Wind Tunnel Simulation Results

NACA Code	Cl at 0°	Cl at 5°	Cl at 10°	Cl at 15°	Cd at 0°	Cd at 5°	Cd at 10°	Cd at 15°
0004	0.00	0.54	1.04	1.32	0.010	0.052	0.161	0.282
0008	0.00	0.56	1.07	1.37	0.012	0.049	0.153	0.288
0012	0.00	0.58	1.11	1.41	0.017	0.022	0.148	0.275
2404	0.25	0.77	1.24	1.49	0.019	0.087	0.218	0.343
2408	0.24	0.79	1.28	1.53	0.018	0.084	0.209	0.333
2412	0.24	0.80	1.31	1.57	0.022	0.086	0.205	0.323
4404	0.48	0.99	1.44	1.65	0.039	0.131	0.280	0.407

4408	0.48	1.00	1.47	1.69	0.035	0.127	0.270	0.382
4412	0.48	1.01	1.50	1.73	0.037	0.128	0.267	0.374
6404	0.71	1.19	1.63	1.81	0.071	0.176	0.334	0.461
6408	0.71	1.21	1.66	1.85	0.066	0.175	0.331	0.438
6412	0.70	1.22	1.69	1.88	0.066	0.178	0.334	0.437

NACA Code	LTD at 0°	LTD at 5°	LTD at 10°	LTD at 15°
0004	0.000	10.570	6.444	4.686
0008	0.000	11.552	7.034	4.745
0012	0.000	11.101	7.488	5.112
2404	12.678	8.813	5.718	4.350
2408	13.451	9.336	6.121	4.595
2412	11.101	9.313	6.381	4.858
4404	12.222	7.526	5.153	4.066
4408	13.647	7.855	5.448	4.426
4412	12.882	7.928	5.611	4.614

6404	10.006	6.797	4.879	3.926
6408	10.663	6.900	5.016	4.215
6412	10.603	6.867	5.042	4.304

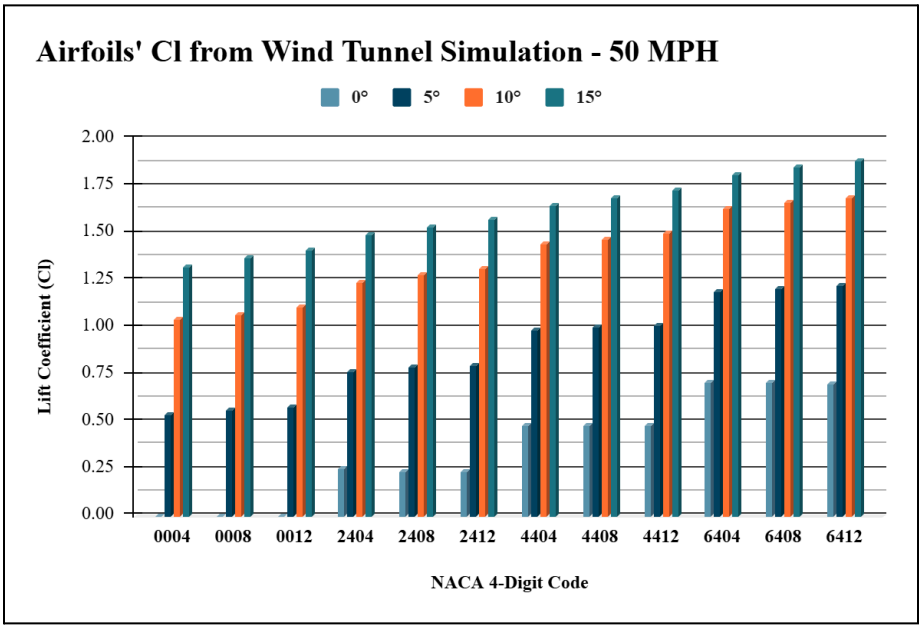

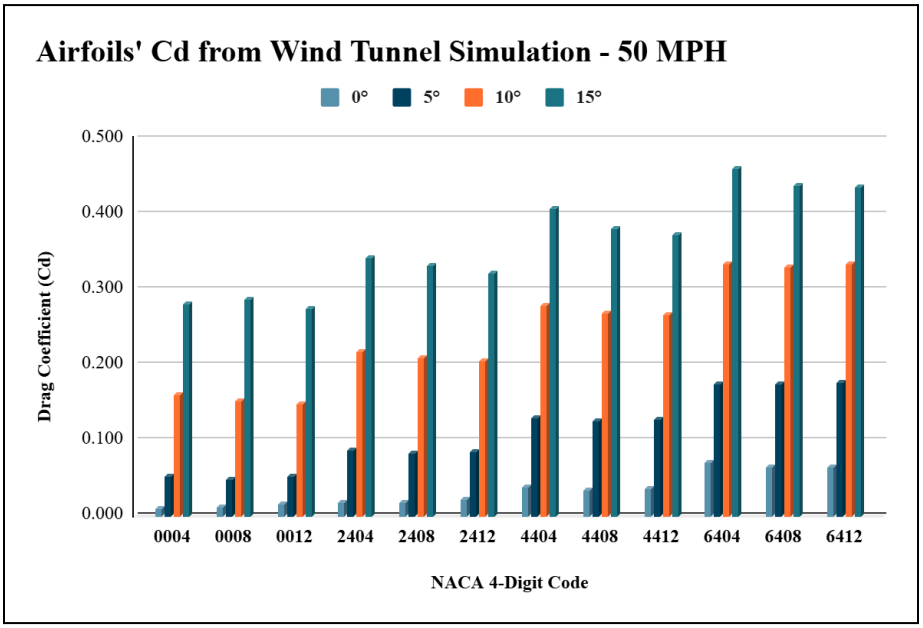

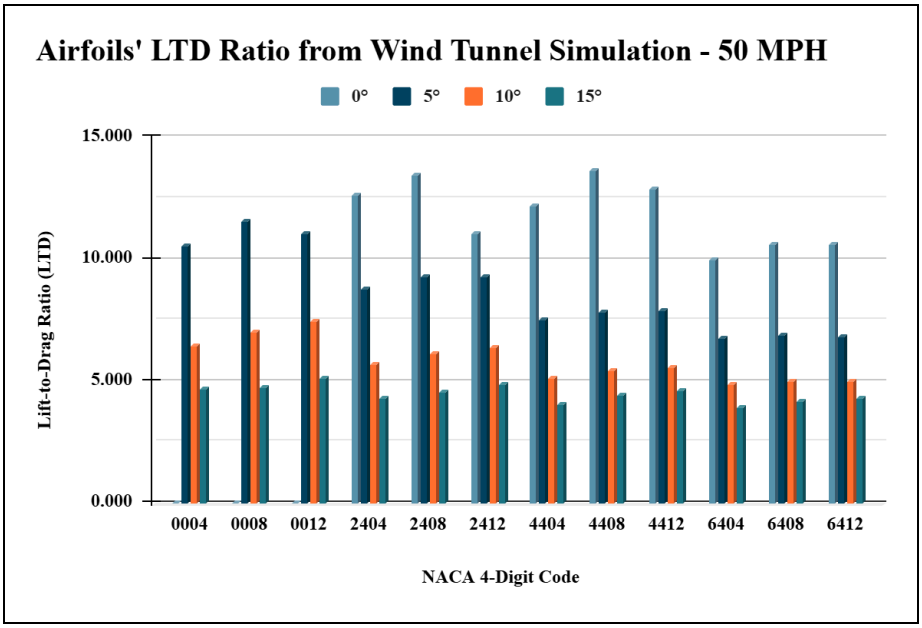

Appendix D: Tables and Graphs From 50 MPH Water Tunnel Simulation Results

NACA Code	Cl at 0°	Cl at 5°	Cl at 10°	Cl at 15°	Cd at 0°	Cd at 5°	Cd at 10°	Cd at 15°
0004	0.00	0.54	1.04	1.32	0.007	0.045	0.148	0.255
0008	0.00	0.56	1.04	1.32	0.009	0.044	0.142	0.262
0012	0.00	0.58	1.11	1.41	0.013	0.047	0.140	0.254
2404	0.25	0.77	1.24	1.49	0.016	0.080	0.201	0.312
2408	0.24	0.79	1.28	1.53	0.015	0.078	0.196	0.307
2412	0.24	0.80	1.31	1.57	0.018	0.080	0.194	0.302
4404	0.48	0.99	1.44	1.65	0.035	0.122	0.260	0.372

4408	0.48	1.00	1.47	1.69	0.032	0.120	0.255	0.356
4412	0.48	1.01	1.50	1.73	0.033	0.121	0.254	0.353
6404	0.71	1.19	1.63	1.81	0.066	0.166	0.315	0.426
6408	0.71	1.21	1.66	1.85	0.062	0.166	0.314	0.411
6412	0.70	1.22	1.69	1.88	0.062	0.169	0.319	0.413

NACA Code	LTD at 0°	LTD at 5°	LTD at 10°	LTD at 15°
0004	0.000	11.828	7.049	5.188
0008	0.000	12.696	7.543	5.218
0012	0.000	12.320	7.896	5.529
2404	15.152	9.624	6.195	4.784
2408	16.002	10.062	6.525	4.988
2412	13.411	10.007	6.721	5.202
4404	13.629	8.097	5.542	4.446
4408	14.981	8.364	5.781	4.754
4412	14.279	8.406	5.899	4.901

6404	10.843	7.196	5.183	4.255
6408	11.456	7.268	5.284	4.496
6412	11.398	7.226	5.291	4.558

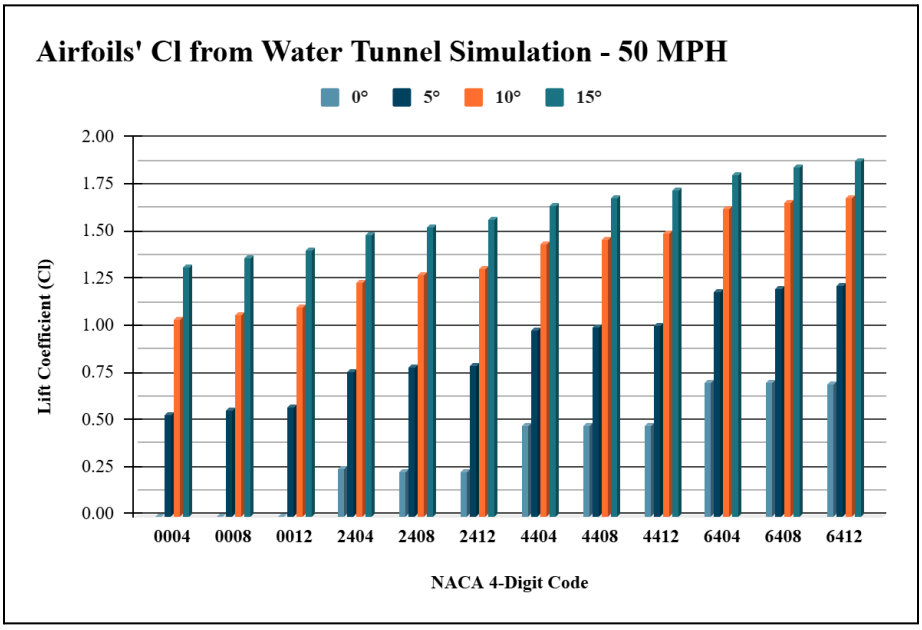

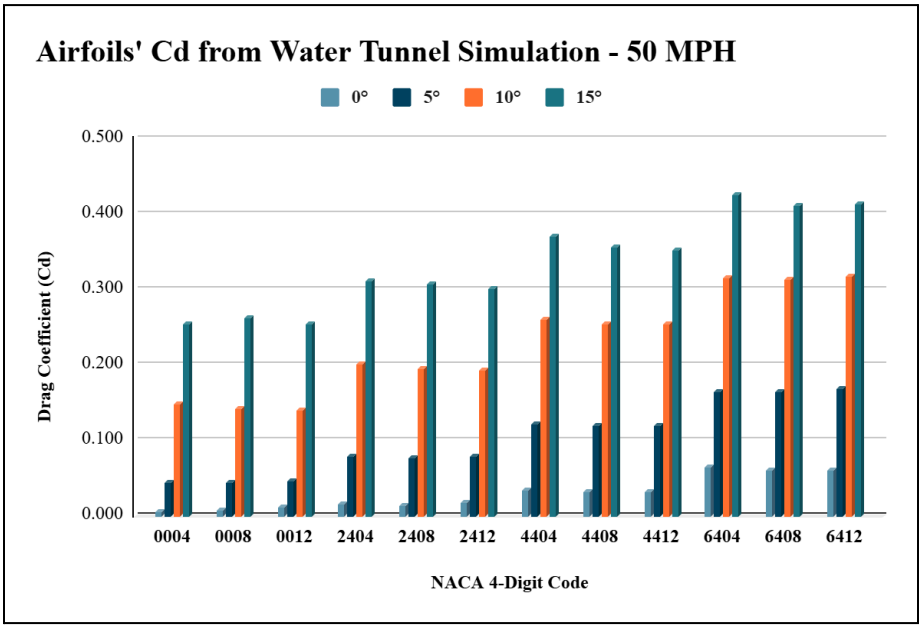

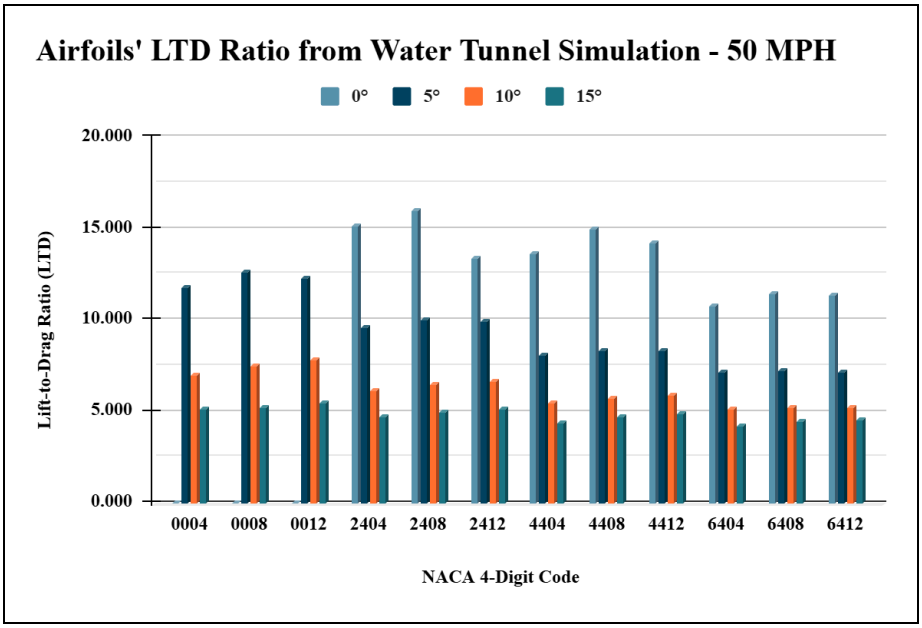

Appendix E: Tables and Graphs From 100 MPH Wind Tunnel Simulation Results

NACA Code	Cl at 0°	Cl at 5°	Cl at 10°	Cl at 15°	Cd at 0°	Cd at 5°	Cd at 10°	Cd at 15°
0004	0.00	0.54	1.04	1.32	0.009	0.050	0.157	0.274
0008	0.00	0.56	1.07	1.37	0.011	0.047	0.149	0.280
0012	0.00	0.58	1.11	1.41	0.016	0.050	0.145	0.268
2404	0.25	0.77	1.24	1.49	0.018	0.085	0.212	0.333
2408	0.24	0.79	1.28	1.53	0.017	0.082	0.204	0.325
2412	0.24	0.80	1.31	1.57	0.021	0.084	0.202	0.316
4404	0.48	0.99	1.44	1.65	0.038	0.128	0.273	0.395

4408	0.48	1.00	1.47	1.69	0.034	0.125	0.265	0.374
4412	0.48	1.01	1.50	1.73	0.036	0.126	0.263	0.367
6404	0.71	1.19	1.63	1.81	0.069	0.173	0.328	0.450
6408	0.71	1.21	1.66	1.85	0.065	0.172	0.326	0.430
6412	0.70	1.22	1.69	1.88	0.065	0.175	0.329	0.429

NACA Code	LTD at 0°	LTD at 5°	LTD at 10°	LTD at 15°
0004	0.000	10.940	6.625	4.835
0008	0.000	11.893	7.189	4.886
0012	0.000	11.542	7.613	5.238
2404	13.374	9.056	5.861	4.480
2408	14.170	9.556	6.244	4.713
2412	11.745	9.523	6.486	4.963
4404	12.637	7.699	5.271	4.179
4408	14.045	8.010	5.550	4.526
4412	13.296	8.074	5.699	4.702

6404	10.258	6.919	4.972	4.025
6408	10.917	7.013	5.098	4.301
6412	10.844	6.977	5.119	4.382

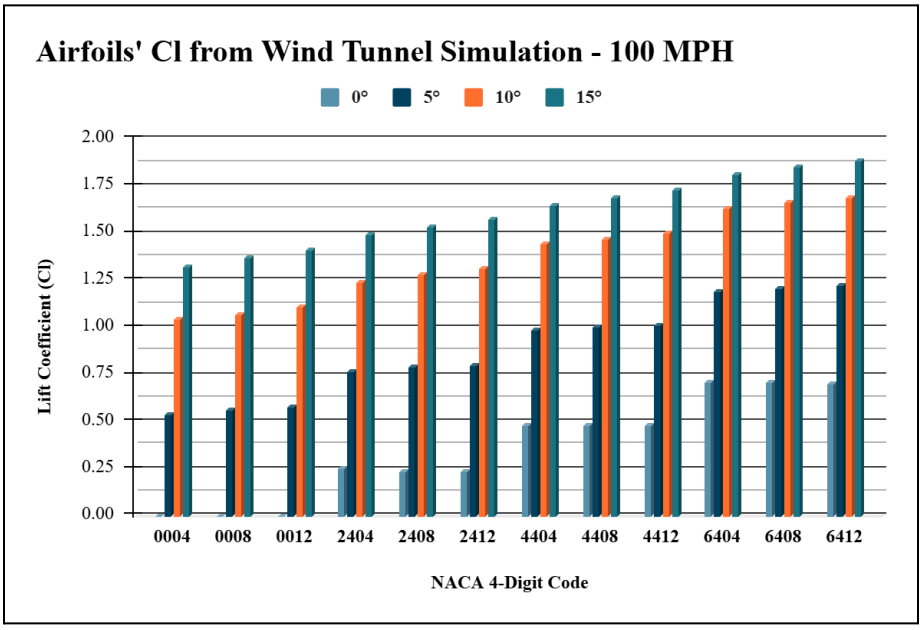

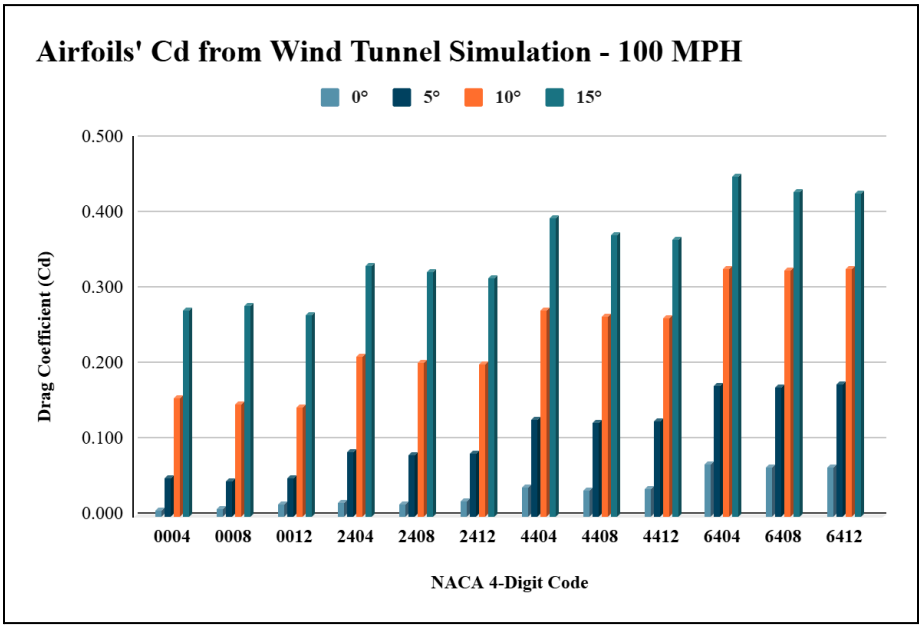

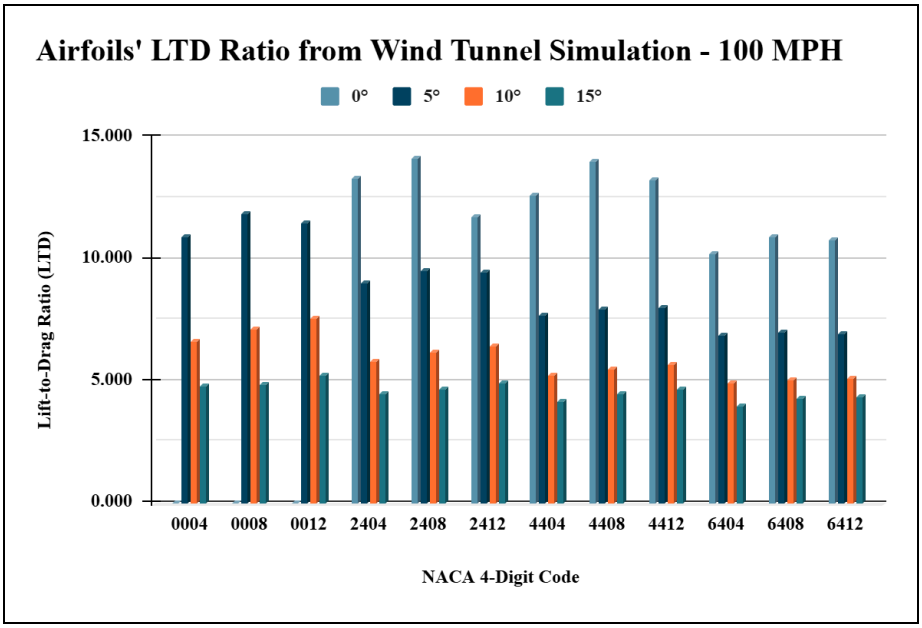

Appendix F: Tables and Graphs From 100 MPH Water Tunnel Simulation Results

NACA Code	Cl at 0°	Cl at 5°	Cl at 10°	Cl at 15°	Cd at 0°	Cd at 5°	Cd at 10°	Cd at 15°
0004	0.00	0.54	1.04	1.32	0.007	0.045	0.144	0.248
0008	0.00	0.56	1.04	1.32	0.008	0.043	0.140	0.255
0012	0.00	0.58	1.11	1.41	0.012	0.046	0.138	0.249
2404	0.25	0.77	1.24	1.49	0.015	0.078	0.197	0.304
2408	0.24	0.79	1.28	1.53	0.015	0.077	0.192	0.301
2412	0.24	0.80	1.31	1.57	0.017	0.079	0.192	0.296
4404	0.48	0.99	1.44	1.65	0.034	0.119	0.255	0.363

4408	0.48	1.00	1.47	1.69	0.031	0.118	0.251	0.349
4412	0.48	1.01	1.50	1.73	0.033	0.119	0.251	0.347
6404	0.71	1.19	1.63	1.81	0.064	0.164	0.310	0.417
6408	0.71	1.21	1.66	1.85	0.061	0.164	0.310	0.404
6412	0.70	1.22	1.69	1.88	0.061	0.167	0.315	0.407

NACA Code	LTD at 0°	LTD at 5°	LTD at 10°	LTD at 15°
0004	0.000	12.183	7.215	5.237
0008	0.000	13.012	7.679	5.349
0012	0.000	12.625	8.002	5.642
2404	15.912	9.846	6.324	4.904
2408	16.782	10.257	6.632	5.094
2412	14.132	10.193	6.810	5.293
4404	14.025	8.250	5.647	4.550
4408	15.348	8.499	5.868	4.842
4412	14.668	8.533	5.975	4.977

6404	11.069	7.301	5.264	4.343
6408	11.662	7.365	5.354	4.571
6412	11.612	7.320	5.356	4.625

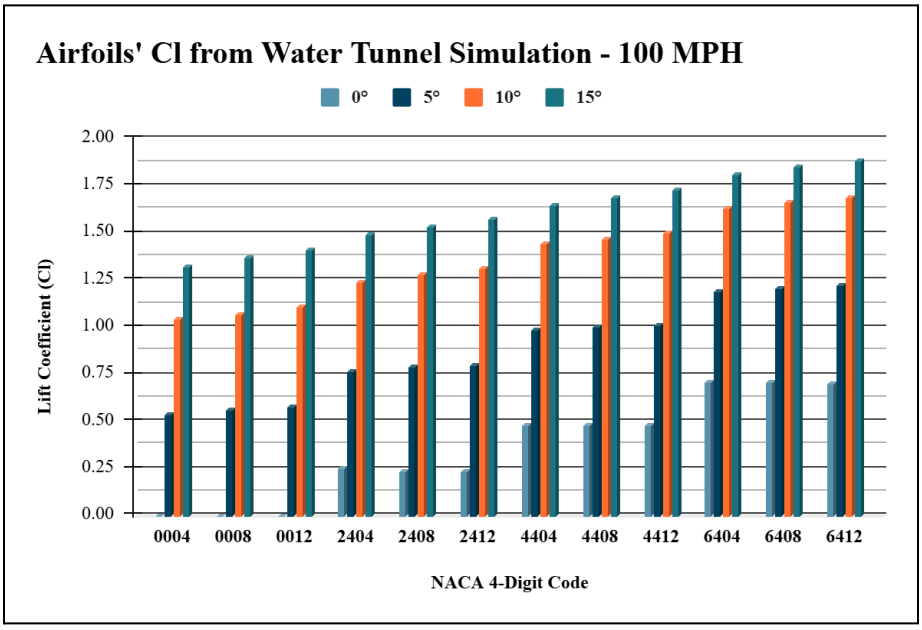

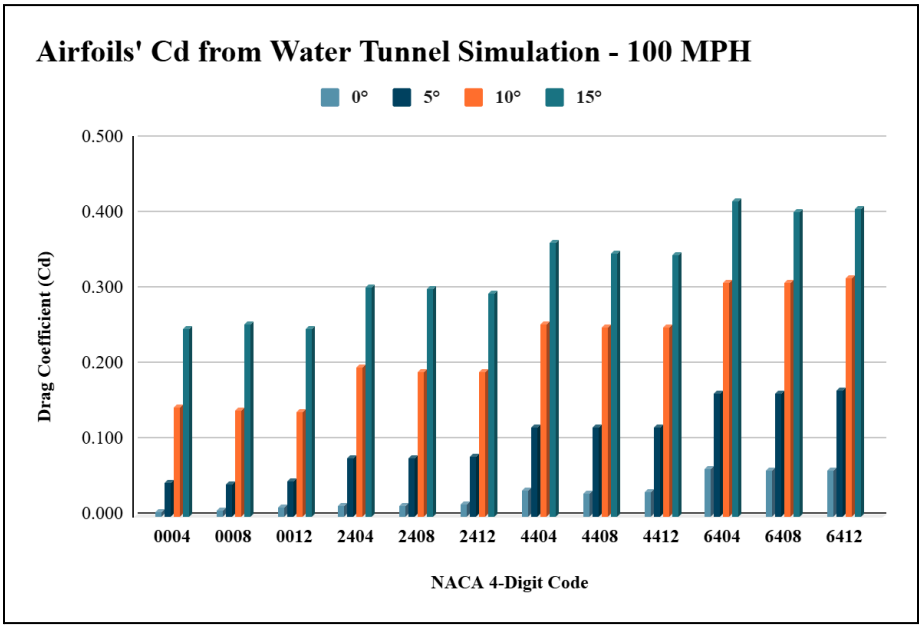

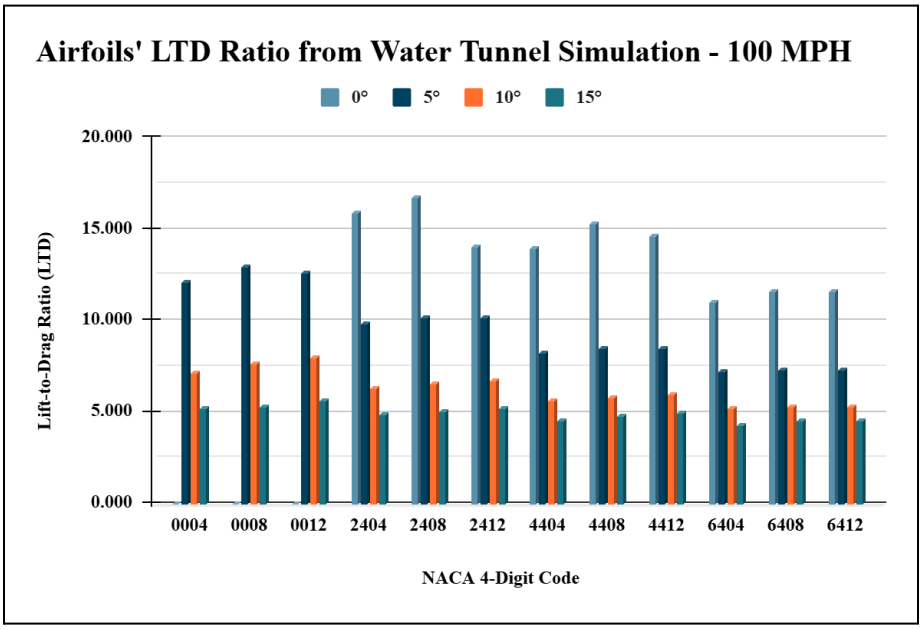
Airfoils' LTD Ratio from Water Tunnel Simulation - 100 MPH
0°
5°
10°
15°
20.000
15.000
10.000
5.000
0.000
Lift-to-Drag Ratio (LTD)
0004
0008
0012
2404
2408
2412
4404
4408
4412
6404
6408
6412
NACA 4-Digit Code